Available online at www.sciencedirect.com
SCIENCE DIRECT
Journal of Catalysis 242 (2006) 184–194
JOURNAL OF CATALYSIS
www.elsevier.com/locate/jcat

Ammonia oxidation on Pt(410)

C.J. Weststrate [a,*], J.W. Bakker [a], E.D.L. Rienks [a], C.P. Vinod [a,b], A.V. Matveev [c], V.V. Gorodetskii [c], B.E. Nieuwenhuys [a,b]

[a] *Leids Instituut voor Chemisch Onderzoek, Universiteit Leiden, P.O. Box 9502, Einsteinweg 55, 2333 CC Leiden, The Netherlands*
[b] *Technische Universiteit Eindhoven, Schuit Institute of Catalysis, P.O. Box 5600 MB, Eindhoven, The Netherlands*
[c] *Boreskov Institute of Catalysis, Russian Academy of Sciences, Novosibirsk 630090, Russia*

Received 19 April 2006; revised 12 June 2006; accepted 13 June 2006

Available online 12 July 2006

Abstract

The adsorption of both O_2 and NH_3 on Pt(410) was studied using temperature-programmed desorption (TPD) and X-ray photoelectron spectroscopy (XPS). Molecular NH_3 desorbed from Pt(410) between 100 and 450 K, and dissociation was not observed. Radiation (X-rays, electrons) induced NH_{3ad} dissociation, and as a result several dissociation products (NH_{2ad}, NH_{ad}, and N_{ad}) were observed in the N 1*s* core-level spectrum. NH_{ad} is a rather stable dissociation product that starts to dehydrogenate above 350 K. The N_{ad} and H_{ad} formed in this process desorbed on formation (as N_2 and H_2). Both molecular and dissociative O_2 adsorption were observed after the surface was exposed to O_2(g) at 100 K. Molecularly adsorbed O_2 desorbed below 200 K, whereas atomic oxygen desorbed (as O_2) between 600 and 900 K, in two distinct desorption peaks. In the O 1*s* core-level spectrum, both molecular O_2 and two different types of O_{ad} were distinguished. NH_{3ad} dissociation was observed on an oxygen-presaturated surface. The NH_{3ad} oxy-dehydrogenation started at 150 K. NO_{ad} and NO(g) were also observed, but only during experiments in which an excess of O_{ad} was available. NO_{ad} desorbed/decomposed between 400 and 500 K. For the steady-state ammonia oxidation reaction, N_2 and H_2O were the major products at low temperatures, whereas the selectivity toward NO and H_2O changed at higher temperatures. This selectivity change can be attributed to changes in surface composition.

Keywords: O_2 adsorption; NH_3; Pt(410); Ammonia oxidation; NO formation; X-ray photoelectron spectroscopy; Synchrotron radiation; Temperature-programmed desorption

1. Introduction

Catalytic ammonia oxidation is an important process in the chemical industry. It is used on a large scale to produce nitric oxide, a precursor for nitric acid. The catalyst of choice for this process is an alloy of Pt and Rh. A number of surface science studies have been performed to unravel the surface chemistry of NH_3 on Pt surfaces in both the absence and presence of co-adsorbed oxygen [1–3].

The surface chemistry of ammonia on a metal surface is complex, involving several different surface species. Adsorption and decomposition of NH_3 can in principle lead to five different species: NH_{3ad}, NH_{2ad}, NH_{ad}, N_{ad}, and H_{ad}. In the presence of oxygen, several other species can are involved in the surface chemistry, including O_{ad}, OH_{ad}, H_2O_{ad}, and NO_{ad}. The complexity of the surface chemistry is reflected in the gas-phase product selectivity during catalytic NH_3 oxidation. Different gaseous products, including N_2, NO, and N_2O, can be formed. The selectivity depends on the type of catalyst, its surface structure, and the experimental conditions, such as reactant pressures, NH_3/O_2 ratio, and catalyst temperature.

It has been found that ammonia decomposition does not take place on Pt surfaces at temperatures below 400 K. Some NH_3 decomposition has been observed *above* the NH_3 desorption temperature; in that case, stepped surfaces were found to be more active than "smooth" surfaces [1,4,5]. On several metals, including Pt, Ag, Ir, and Cu, the presence of oxygen has been found to enhance NH_3 dissociation [3,6–11].

In this paper we present the results obtained for ammonia oxidation on a Pt(410) surface, which consists of {100} terraces

* Corresponding author.
E-mail address: c.westrate@chem.leidenuniv.nl (C.J. Weststrate).

0021-9517/$ – see front matter
doi:10.1016/j.jcat.2006.06.011

and {110} steps. Faceting of the surface was observed, resulting in the formation of larger {100} terraces on which a (5 × 20) reconstruction occurred. A more detailed discussion concerning the actual surface structure of our Pt(410) sample has been provided previously [12].

XPS was used to study the nature and concentration of surface species, and the gas-phase reaction products were detected by quadrupole mass spectrometry (QMS). The aim of our experiments was to obtain fundamental insights into surface processes, which can help elucidate the reaction pathways involved in catalytic ammonia oxidation. Based on our previous studies, we also can compare the NH_3 chemistry on Pt(410) with that on (previously studied) Ir surfaces [9,13–16].

2. Experimental

The thermal desorption studies were performed using the experimental setup in Leiden, which has been described in more detail elsewhere [12]. High-energy resolution fast XPS measurements [17,18] were performed on the SuperESCA beamline of ELETTRA, the synchrotron radiation facility in Trieste, Italy. The vacuum system, with a base pressure of $\sim 1 \times 10^{-10}$ mbar, is equipped with a sputter ion gun for sample cleaning, a mass spectrometer, and LEED optics. Details about the sample used in this study and the cleaning procedure can be found elsewhere [12].

The N 1*s* spectra were measured with a photon energy of 496 eV, and the O 1*s* spectra were measured with a photon energy of 650 eV. Temperature-programmed XPS (TP-XPS) measurements [19] were performed at a heating rate of 0.25 K s^{-1}. The different core level regions were measured in a separate experiment; that is, either O 1*s* or N 1*s* could be measured during an experiment. The XPS spectra were evaluated after a linear background was subtracted by fitting the peaks with a Doniach–Šunjić function convoluted with a Gaussian function [20].

Core-level binding energies of the different species were measured with respect to the Fermi level. The position of the Fermi edge was determined using an photon energy of 110 eV. In recent experiments, we found that the position of the Fermi level should be measured using the photon energy used for the actual measurements as well, because the calibration of the photon energy was not very accurate (e.g., when the excitation energy was set to 650 eV, the *actual* energy was ∼647 eV). As a result of the approach used here (i.e., measuring the Fermi edge with a different photon energy than for the actual measurements), the reported *absolute* binding energies (BEs) can exhibit a (constant) shift with respect to literature values. Therefore, the ΔBEs between different species instead of *absolute* BEs should be used for comparison with literature data. This issue affected only the comparison with literature data; the position of the different species remained constant throughout the experiments. The N 1*s* and O 1*s* signals were normalized using the intensities obtained for a saturated NO layer at 100 K (which was arbitrarily set to 1).

Both Sun et al. [21] and Schwaner et al. [22] found that adsorbed NH_3 decomposed when exposed to a beam of (∼50 eV) electrons. In the experimental setup used for the thermal desorption experiments, radiation damage due to electrons from the QMS filaments (∼70 eV) can be excluded, because the QMS was situated in a separate compartment, with only a small hole connecting it to the main chamber (where the crystal was located). In this setup, the likelihood of electrons generated by the QMS filaments reaching the sample surface is very low. During the XPS measurements, NH_{3ad} dissociation was induced by the intense radiation (either X-rays or ∼100 eV photoelectrons). This is described in more detail in Section 3.1.

3. Results

3.1. NH_3 surface chemistry

Thermal desorption spectra obtained after exposure to NH_3 at 100 K are shown in Fig. 1a. Ammonia bonded directly to the surface (through the nitrogen atom) desorbed molecularly between 200 and 450 K. After an NH_3 exposure of ∼3 L, a new desorption feature appeared, with a desorption maximum at around 175 K. In line with literature assignments, this peak can be attributed to desorption of a second NH_3 layer that was hydrogen-bonded to the first, chemisorbed layer [5,13,23–26]. Even higher exposures led to the formation of NH_3 multilayers that desorbed at around 120 K [5,27]. The observed peaks are very similar to the desorption spectra observed for other Pt surfaces, and the presence of steps seemed to have little effect on the desorption spectra. N_2 or H_2 desorption was not observed, indicating that NH_3 dissociation did not take place on the clean surface.

Fig. 2a shows one of the N 1*s* core-level spectra obtained during XPS experiments of an adsorbed $NH_3/NH_{x\mathrm{ad}}$ layer. It also shows the fitting components used to deconvolute the spectra. The BEs of all of the fitting components used to evaluate the XPS data are summarized in Table 1. Fig. 2b shows a series of spectra taken during heating of an adsorbed $NH_3/NH_{x\mathrm{ad}}$ layer in vacuum. Ammonia was dosed at 175 K, to avoid formation of the NH_3 double layer. During the uptake (not shown), initially only molecular ammonia was observed (at 400 eV). However, the intense radiation (either X-rays or the resulting ∼100-eV photoelectrons) induced dissociation of the adsorbed NH_3, and another peak developed at 398.3 eV, assigned to NH_{ad}. We suggest that another small peak was present at 399.1 eV, which is assigned to $NH_{2\mathrm{ad}}$ on the basis of its BE. This peak was never clearly resolved, and the concentration of this species was low. Heating of the dissociated $NH_{x\mathrm{ad}}$ layer (Figs. 1c and 2b) resulted in the formation of an additional (small) peak at 397.4 eV, assigned to N_{ad}. This assignment is in line with literature data [8,13,21] in which the ΔBE among various $NH_{x\mathrm{ad}}$ species was reported to be ∼1 eV on several different metal surfaces. The same BE component was observed after NO dissociation on this surface [12]. Fig. 1c shows the results obtained after evaluation of the data shown in Fig. 2b using the components shown in panel (a). $NH_{3\mathrm{ad}}$ desorbed between 175 and 400 K, and $NH_{2\mathrm{ad}}$ decomposed (into NH_{ad} and H_{ad}) between 175 and 250 K. NH_{ad} decomposition was observed above 350 K. As a result, a small amount of N_{ad} that desorbed almost immediately on formation (as N_2) was observed.

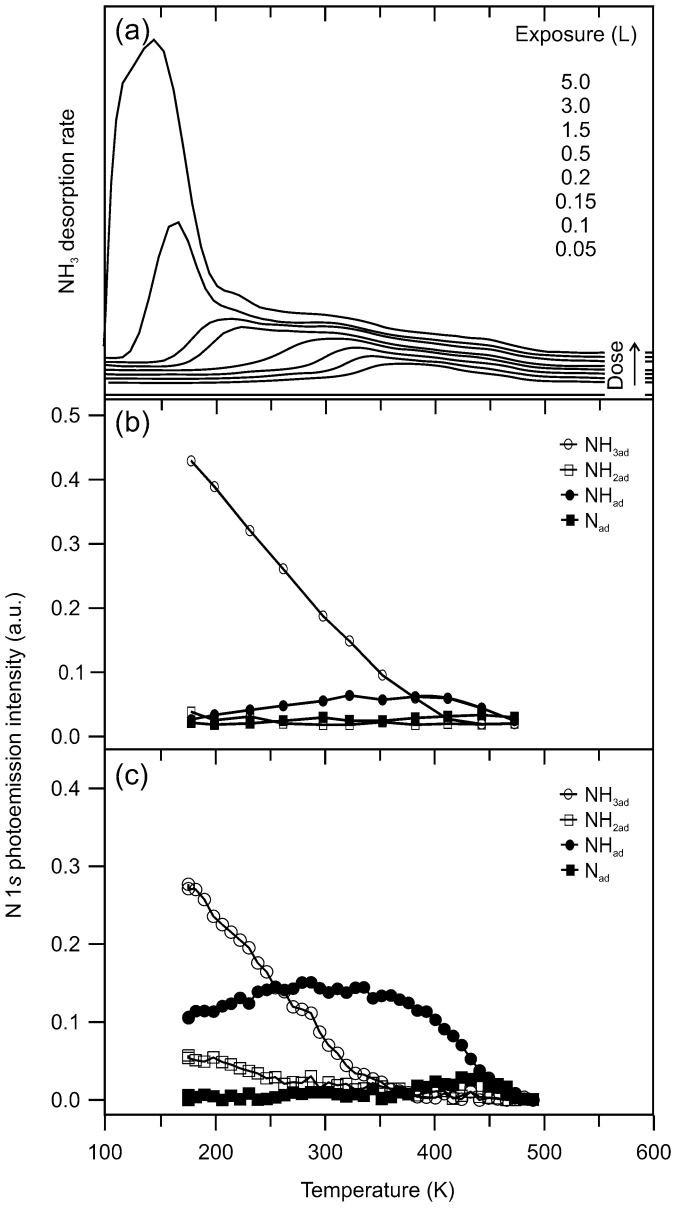

Fig. 1. (a) NH_3 desorption after exposure to ammonia at 100 K (3 K s^{-1}). (b) TP-XPS results obtained during heating of an adsorbed NH_3 layer (0.25 K s^{-1}, exposed to NH_3 at 175 K). The exposure to the X-rays was kept as low as possible. (c) Thermal behavior of NH_3 dissociation products (formed by radiation damage) on Pt(410) (0.25 K s^{-1}).

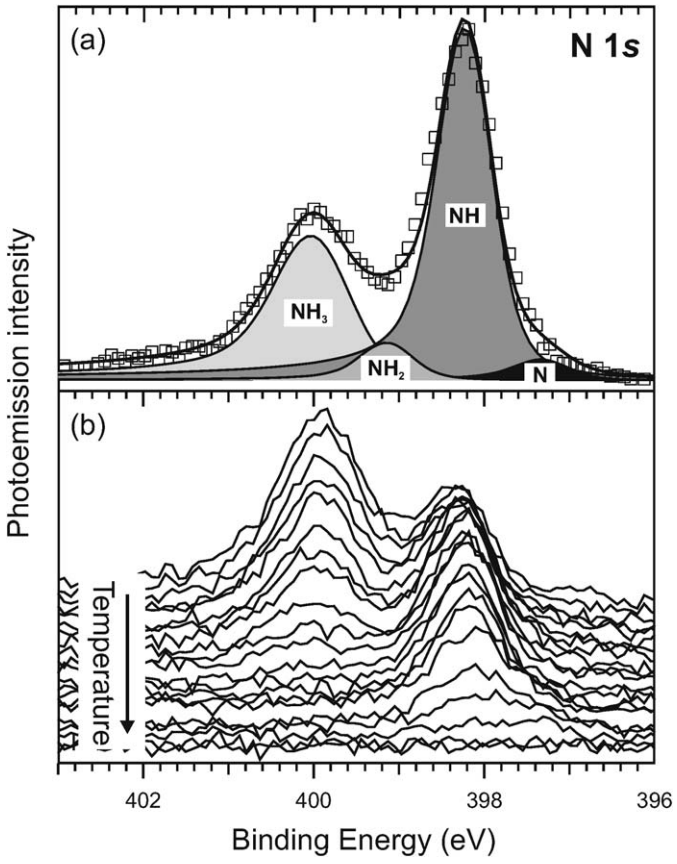

Fig. 2. (a) Components used to fit the N 1*s* spectra obtained during experiments with ammonia (average of three spectra). (□) Datapoints, (—) fit. (b) The actual spectra observed during heating (0.25 K s^{-1}) of an irradiated NH_{3ad} layer. Radiation damage causes the formation of NH_{xad} ($x = 0, 1, 2$).

Table 1
Binding energies found for NH_3, NO and O_{ad} adsorption on Pt(410)[a]

Assignment	N 1*s* BE (eV)	O 1*s* BE (eV)
NH_{3ad}	400.0	–
NH_{2ad}	399.1	–
NH_{ad}	398.3	–
N_{ad}	397.4	–
NO_{ad}	400.7	533.0
O_I	–	530.8
O_{II}	–	531.7
O_2	–	532.4
H_2O_{ad}	–	534.2
CO_{ad}	–	534.1

[a] See Section 2 for more details about the calibration.

The data presented in Fig. 1b differ drastically from that shown in Fig. 1c. In the experiment presented in panel (c), the surface was already exposed to radiation during exposure to NH_3, and it was also continuously exposed to the X-rays during heating. As a result, the concentration of dissociated species was high. For the experiment presented in Fig. 1b, the NH_3 uptake was done in the absence of radiation, and during heating the number of data points was kept low, to minimize the radiation dose (each marker represents one data point, ∼30 s). When the experiment was done it this way, NH_3 dissociation was almost absent, in line with the TPD data. This shows that radiation has a profound effect on the surface chemistry of NH_{3ad}, and confirms that NH_3 dissociation did not occur on the Pt(410) surface (*in the absence of radiation*).

3.2. Characterization of the oxygen-covered surface

Because no literature reports on O_2 adsorption on Pt(410) are available, here we report a brief investigation of oxygen adsorption on Pt(410). Fig. 3 shows several O 1*s* core-level spectra of an oxygen-saturated (O_{2ad}/O_{ad}) Pt(410) surface (10 L, 100 K), during both heating in vacuum [panels (b–d)] and heating in the presence of H_2 [panel (a)]. Fig. 4 shows the thermal

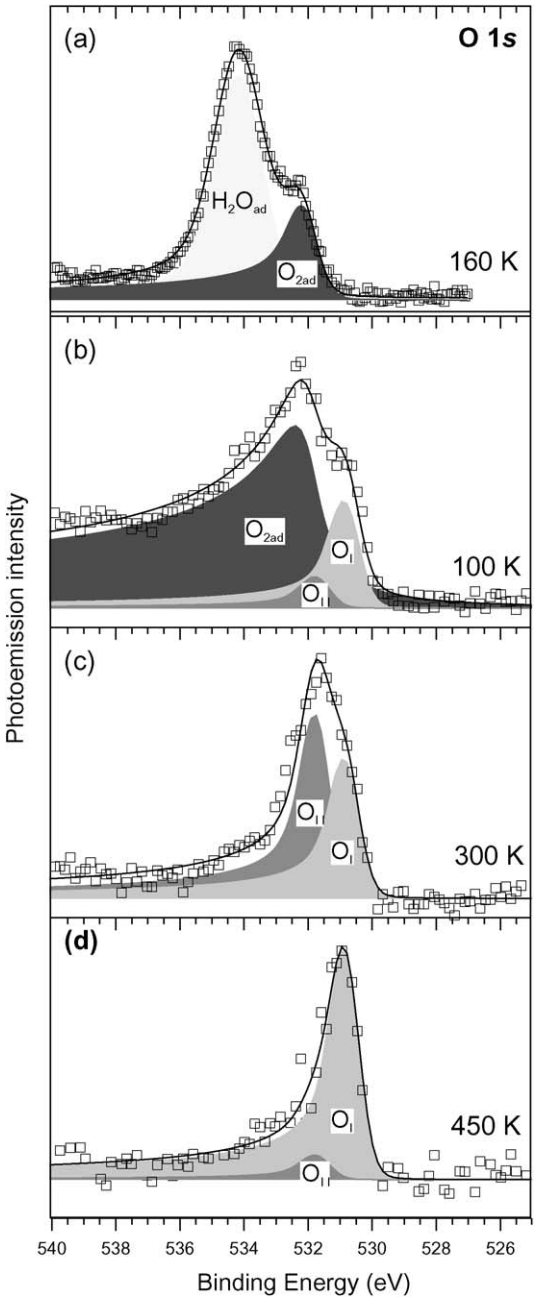

Fig. 3. XP-spectra taken during (a) heating of an adsorbed O_{2ad}/O_{ad} layer in the presence of H_2 (0.25 K s^{-1}, 1×10^{-7} mbar H_2) and (b, c, d) during heating (0.25 K s^{-1}) of a adsorbed O_{2ad}/O_{ad} layer in vacuum.

behavior of the different O 1*s* components in more detail. Panel (a) shows the thermal desorption of O_2 during heating of an oxygen-saturated surface in vacuum, and panel (b) shows the corresponding TP-XPS results. The results shown in panel (c) were obtained during TP-XPS of an O_2-saturated surface in the presence of 1×10^{-7} mbar H_2.

Molecularly adsorbed O_2 was stable only at low temperatures and was observed as a broad, asymmetric peak at 532.4 eV. During O_2 uptake (not shown) at 100 K, both O_{ad} and O_2 grew simultaneously. O_{2ad} desorbed/dissociated at around 150 K and was not observed above 200 K. Freyer et al. [28] reported the BEs for both O_{2ad} and O_{ad} on Pt(110)-(1×2).

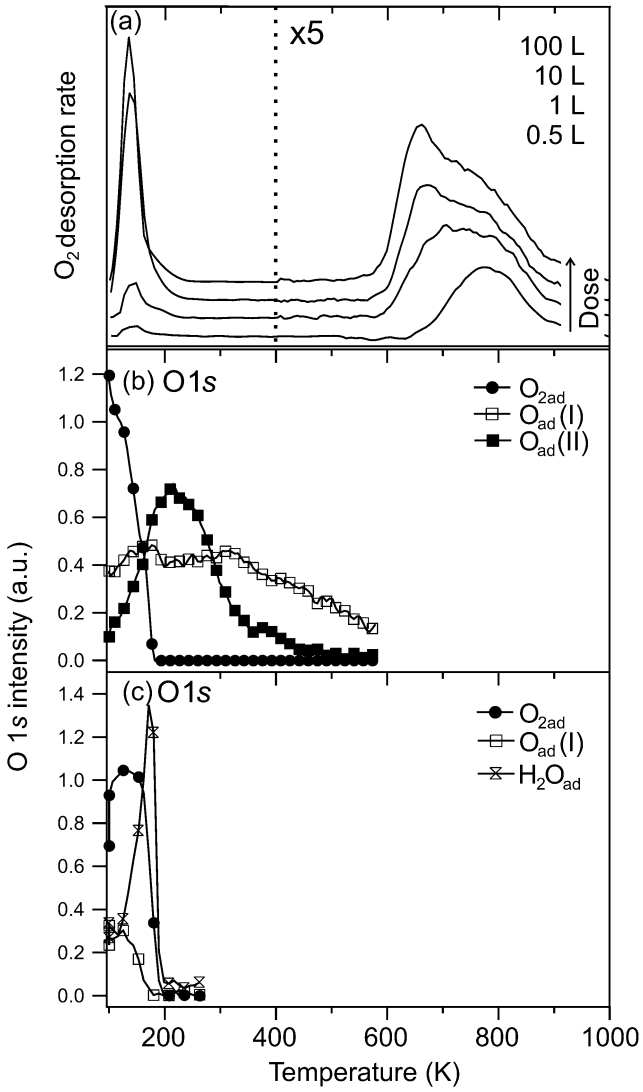

Fig. 4. (a) Oxygen desorption from Pt(410) after exposure to O_2 at 100 K (3 K s^{-1}). (b) Thermal behavior of different oxygen species during heating of an adsorbed O_{2ad}/O_{ad} layer in vacuum (0.25 K s^{-1}) and (c) heating of an adsorbed O_{2ad}/O_{ad} layer in H_2 (0.25 K s^{-1}, 1×10^{-7} mbar H_2).

O_{2ad} was observed at 530.7 eV, whereas O_{ad} was observed at 529.9 eV. Their BEs do not exactly match the values that we obtained,[1] but the ΔBE between O_{2ad} and O_{II} was ∼0.8 eV in both cases.

Above 200 K, two peaks can be distinguished, at 530.8 eV (O_I) and 531.7 eV (O_{II}), both of which are assigned to O_{ad}. The O_I species already formed at 100 K during exposure to O_2, whereas O_{II} was formed during O_{2ad} decomposition at around 150 K. During the slow heating (0.25 K s^{-1}) used in the TP-XPS experiment, O_{II} was consumed via reaction with gases from the background (H_2 and CO), whereas O_I began to react when O_{II} was removed. This indicates that O_{II} is slightly more reactive than O_I.

The O_2 thermal desorption spectra *above* 200 K (i.e., via O_{ad} combination) show two distinct high-temperature desorp-

[1] See Section 2 for details.

tion features, the first at around 670 K and the second at around 800 K. For thermal desorption from other stepped Pt surfaces, like (533) [29,30] two high-temperature O_2 desorption peaks were observed as well, whereas only a single high-temperature O_2 desorption peak was found for the low-index planes [31–33]. This suggests that the origin of the two desorption peaks is related to the presence of steps. It may be that these two distinct O_2 desorption peaks correspond to the two O_{ad} species observed by XPS. The XPS measurements were limited to 600 K, and thus this assignment could not be validated.

During heating of an adsorbed O_{2ad}/O_{ad} layer in the presence of H_2(g), an additional species was observed in the O 1*s* spectrum, between 100 and 200 K, with a BE of 534.2 eV. The fact that it appeared in the presence of H_2 (/H_{ad}) suggests that it was either OH_{ad} or H_2O_{ad}. The ΔBE of 2.5 eV between this species and O_{II} corresponded to the shift observed between O_{ad} and H_2O_{ad} on Pt(111) [34,35]. Kiskinova et al. [36] reported a 1-eV shift between O_{ad} and OH_{ad} on Pt(111). In contrast, EELS experiments on Pt(111) [3] indicated that OH_{ad} formed during NH_{3ad} dehydrogenation and that was stable up to 285 K, so this is another possibility. We tentatively assign this peak to H_2O_{ad} on the basis of the BE, but we cannot exclude the possibility that it was OH_{ad} rather than H_2O_{ad}.

3.3. The effect of O_{ad} on the NH_3 surface chemistry

Fig. 5 shows the results obtained during heating of an oxygen-saturated surface (10 L at 200 K), postdosed with NH_3 (3 L). Panel (a) shows the gas-phase products observed during heating (3 K s^{-1}). Molecular NH_3 desorption was found between 110 and 450 K, with a peak at around 150 K (second NH_3 layer) and a broad desorption region between 150 and 450 K. H_2O desorption occurred between 200 and 350 K. A small amount of N_2 formation (observed for both $m/e = 28$ and 14) was already found at around 200 K, but the largest part of the N_2 desorption was observed between 350 and 500 K. NO formation was not observed in this particular experiment. The conditions under which it forms are discussed in Section 3.4. Similar experiments have been performed by Mieher and Ho [3] for Pt(111), who found N_2 desorption between 400 and 600 K on Pt(111), somewhat higher than in our experiment, in which a part of the N_2 desorption occurs already at around 200 K, and above 500 K N_2 desorption was no longer observed; that is, N_2 desorption (via N_{ad} combination) occurred at a lower temperature on Pt(410).

Figs. 5c and 5d show the TP-XPS results obtained during a similar experiment. We took great care to avoid beam damage during the experiments and checked the influence of the radiation on the outcome of the experiments. The effect of the radiation was negligible in the results presented here. For the N 1*s* spectra, we dosed NH_3 at 175 K, to avoid the formation of either a second NH_3 layer or NH_3 ice, which can obscure the N 1*s* spectra [13]. For the O 1*s* spectra, we dosed NH_3 at 100 K, and in this experiment the second NH_3 layer was formed. Desorption of this layer, which partly blocks the signal from the O_{ad} layer underneath, explains the increase in the O_{ad} signal between 100 and 150 K. Starting at 100 K allowed

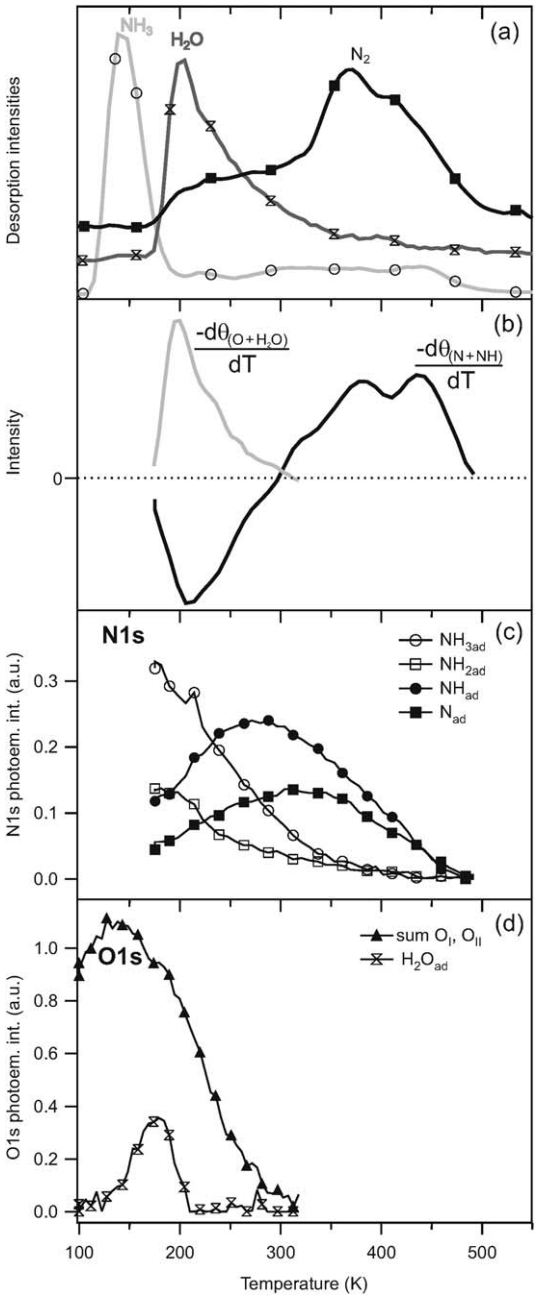

Fig. 5. (a) NH_3, H_2O and N_2 desorption observed during heating of a co-adsorbed NH_{3ad}/O_{ad} layer (3 K s^{-1}). (b) The derivative of the XPS data (similar to thermal desorption spectra). (c) Intensities of the different N 1*s* components obtained during heating of a co-adsorbed NH_{3ad}/O_{ad} layer (0.25 K s^{-1}). (d) Intensities of the different O 1*s* components obtained during heating of a co-adsorbed layer (0.25 K s^{-1}).

us to observe the onset of H_2O_{ad} formation and thus the onset of NH_{3ad} dehydrogenation, which was found to occur already around 150 K. About 40% of the O_{ad} initially present formed H_2O_{ad} below 200 K, whereas the remaining 60% reacted between 200 and 300 K, forming H_2O(g). We did not observe OH_{ad} formation, but this is not surprising, because calculations performed by Offermans et al. [Pt(111)] showed [37], that OH_{ad} species are more reactive than O_{ad} and immediately react with NH_{xad} species to form H_2O_{ad}. In the N 1*s* spectra several NH_{xad} species were already present at the start of the experi-

ment at 175 K (because the reaction between O_{ad} and NH_{3ad} already occurred at around 150 K).

The NH_{3ad} concentration was found to decrease between 175 and 400 K, due to both decomposition and desorption. The NH_{2ad} concentration also decreased between 150 and 250 K, and its concentration was very low above 300 K. Both the N_{ad} and NH_{ad} concentrations increased between 175 and 300 K (due to NH_{3ad} and NH_{2ad} decomposition) and decreased again above 300 K (NH_{ad} dehydrogenated to N_{ad}, which desorbed as N_2). Because both N_{ad} and NH_{ad} were present at the N_2 desorption temperature, we cannot exclude the possibility that N_2 formation involves N_2H_x species.

The presence of NH_{ad} above 300 K, after all of the O_{ad} was consumed, seems to contradict the thermal desorption data. Decomposition of this NH_{ad} (in the absence of O_{ad}) should result in the formation of H_2, but this was not observed in the TPD experiment. However, during heating of an O_{ad} layer in vacuum, we found (see Section 3.2) that O_{ad} was slowly removed by reaction with H_2 and CO from the residual gas. Due to the low heating rate (0.25 K s^{-1}) used in the TP-XPS, much O_{ad} will be removed in this way, leaving less O_{ad} available to react with the remaining NH_{ad}. In the TPD experiment, the heating rate was about 10 times higher (i.e., 3 K s^{-1}), and thus O_{ad} removal by reaction with residual gases played only a minor role.

The XPS results can be used to calculate the thermal desorption spectra. The TPD signal corresponds to $-d\theta/dT$, and by differentiating the $\theta(T)$ signals found with XPS, the thermal desorption spectra can be "calculated." This is a useful method for comparing the TP-XPS and TPD results. The differentiated θ_{O+H_2O} signal [Fig. 5b] was found to be very similar to the H_2O formation observed in the gas phase. This shows that the results found for TPD and TP-XPS are very similar, even though the experimental conditions were different (i.e., different heating rates). The differentiated $(\theta_{NH} + \theta_N)$ signal *below* 300 K shows that NH_{ad} and N_{ad} formed at the same temperature as H_2O(g), whereas the differentiated $(\theta_{NH} + \theta_N)$ signal *above* 300 K matches the N_2 desorption observed in the gas phase; that is, the N_2 desorption peak was a result of desorption of N_{ad} (and decomposition of NH_{ad}) already present on the surface at 300 K.

3.4. N_2 vs. NO formation

A recent publication [12] discussed the surface chemistry of NO on Pt(410). In the N 1*s* spectra, two types of NO, with N 1*s* BEs of 400.7 and 401.3 eV, were observed. In the O 1*s* spectra, only one species was observed, at 533.0 eV. In some of the experiments with ammonia and oxygen, the formation of NO_{ad} was also observed. The peak due to NO_{ad} appeared at 400.7 eV in the N 1*s* region and at 533 eV in the O 1*s* region.

Mieher and Ho [3] showed that NO formation on Pt(111) depends strongly on the amount of available O_{ad} compared with the amount of NH_{3ad} present. They reported the formation of NO(g), but only when the surface was precovered with a large amount of O_{ad} and subsequently exposed to a relatively small amount of NH_3. This observation was rationalized by the following mechanism: Most O_{ad} is consumed *during* NH_{3ad} dehydrogenation (forming H_2O), and NO can be formed only when O_{ad} remains after NH_{xad} dehydrogenation, that is, when the amount of NH_{3ad} is small compared with the amount of O_{ad}.

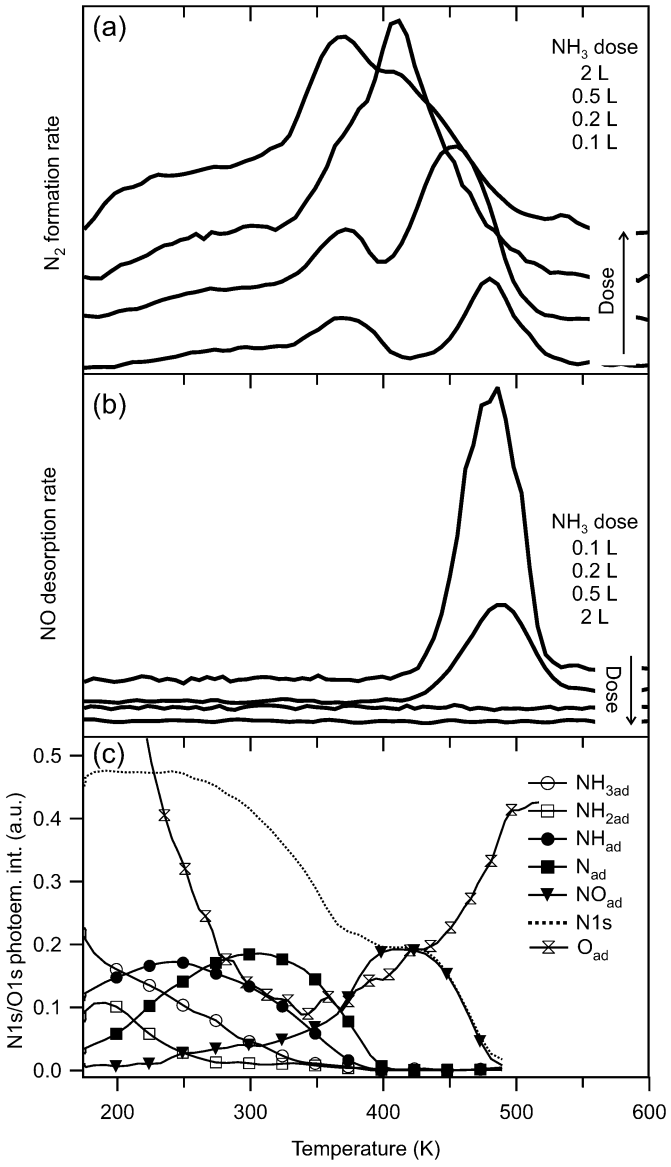

Fig. 6. (a) N_2 formation during heating of an O_{ad} saturated surface (10 L) after different NH_3 post-exposures (3 K s^{-1}). (b) NO formation during heating of an O_{ad} saturated surface (10 L) after different NH_3 post-exposures (3 K s^{-1}). (c) N 1*s* and O 1*s* components during heating of a co-adsorbed NH_{3ad}/O_{ad} layer (0.25 K s^{-1}) in the presence of 5×10^{-8} mbar O_2. The O_{ad} signal shown is the sum of O_I and O_{II}.

A similar trend was observed on Pt(410). Figs. 6a and 6b show both N_2 and NO desorption after exposure of an oxygen-saturated surface (10 L at 200 K) to different amounts of NH_3. Similar to Pt(111), NO desorption occurred only after small doses of ammonia (0.1–0.2 L). N_2 formation observed in a TPD experiment after these low NH_3 doses shows *two* maxima at around 350 and 450 K. We suggest that these different peaks originated from two different mechanisms. The oxygen remaining on the surface after NH_{3ad} dehydrogenation reacted with N_{ad} to form NO_{ad} between 200 and 400 K. The N_{ad} that did not react with O_{ad} desorbed as N_2 at around 350 K. This ex-

plains the first N_2 desorption peak. NO_{ad} decomposition started at above 400 K [12], and the N_{ad} formed in this process desorbed as N_2 at around 450 K, the second N_2 desorption peak. A similar reaction scheme was proposed by Bradley et al. [11] for Pt(100).

This specific experiment was difficult to reproduce during the TP-XPS measurements (due to reaction of O_{ad} with background gases); thus, a different approach was adopted. An O_2 uptake experiment (not shown) on a NH_{3ad}-saturated surface (at 175 K) revealed that O_2 could access the surface and dissociate, even in the presence of a saturated NH_{3ad} layer. We drew on this finding in an attempt to make NO_{ad}. In this particular experiment, a mixed O_{ad}/NH_{3ad} layer was heated in the presence of 5×10^{-8} mbar O_2. Here O_2 could replenish the O_{ad} consumed during NH_{xad} dehydrogenation, and as a result O_{ad} was present throughout the experiment. Fig. 6c shows the results of this experiment, as observed with XPS.

Comparing these results with those of a similar experiment in the *absence* of O_2(g) but in the presence of O_{ad} (see Fig. 5) reveals several differences. The NH_{ad} concentration decreased at a lower temperature in the presence of O_2(g), due to the fact that in this experiment more O_{ad} was available and NH_{ad} could be completely dehydrogenated via reaction with O_{ad}. The formation of NO_{ad} was observed only in the presence of O_2(g). This finding is in line with the model presented in the previous paragraphs; that is, NO_{ad} could form only when O_{ad} was available after all NH_{xad} was dehydrogenated.

The differentiated total N 1*s* signal ($\theta_{NH_x} + \theta_N + \theta_{NO}$, not shown) corresponds rather well to the TPD results obtained using a low NH_3 postexposure; the decreased N 1*s* intensity between 300 and 350 K corresponds to the first N_2 desorption peak. A part of the N_{ad} formed NO_{ad}, which desorbed/decomposed between 400 and 500 K. NO_{ad} can be clearly observed in both the N 1*s* and O 1*s* region above 400 K, where it was the only species (next to O_{ad}) present. Below 400 K, determining the exact intensity of the NO_{ad} peak is more difficult, due to the fact that other species (especially NH_{3ad}) overlapped with the NO_{ad} peak. Therefore, the exact temperature at which NO_{ad} formation started cannot be determined. From spectra obtained during steady-state NH_3 oxidation (see Section 3.5), we tentatively conclude that NO_{ad} formation started already at around 200 K. Reflection absorption infrared spectroscopy (RAIRS) experiments done by Kim et al. [38] showed that NO_{ad} formation on Pt(100) started at around 275 K.

From the XPS data, we cannot distinguish NO_{ad} decomposition from NO_{ad} desorption, because N_{ad} formed during dissociation immediately desorbed as N_2 and was not observed on the surface. The fact that the NO_{ad} concentration dropped at around 450 K and *not* at around 400 K, the temperature at which NO_{ad} decomposition started (see Ref. [12]), indicates that NO_{ad} desorbed rather than decomposed. Experiments done by Bradley et al. on Pt(100) indicated that a high O_{ad} concentration inhibited NO_{ad} dissociation [11]. In our experiment, we found a rather high O_{ad} concentration at around 450 K, so it is very well possible that it blocked NO_{ad} dissociation and that the decreased NO_{ad} was due to desorption rather than to dissociation.

3.5. Steady-state NH_3 oxidation on Pt(410)

Fig. 7 shows the results obtained during steady-state NH_3 oxidation (ratio 1:1). Panels (a) and (b) show the gas-phase products, and panels (c) and (d) and (e) and (f) show the N 1*s* and O 1*s* components, respectively. Both the results obtained during heating [(a), (c), and (e)] and during subsequent cooling [(b), (d), and (f)] are shown. The surface was saturated with O_{ad} (10 L O_2, 200 K) before being exposed to the reaction mixture.

At 250 K, the surface was covered with a mixture of NH_{3ad} ($+NH_{2ad}$), NH_{ad}, N_{ad}, and NO_{ad}. The concentrations of NH_{3ad} ($+NH_{2ad}$), NH_{ad}, and N_{ad} decreased with increasing temperature. The adsorption of O_2 from the gas phase seemed to be hindered by the NH_{xad} species present on the surface, and all O_{ad} that formed on the surface immediately reacted with NH_{xad} species. This explains why the O_{ad} concentration remained low.

NO_{ad} formation was already observed around 250 K. In the N 1*s* spectrum, the peak due to NO_{ad} was not very well resolved, due to the presence of several other N-containing species (especially NH_{3ad}), but it was clearly observed in the O 1*s* spectra, being the only peak present at this temperature. The amount of NO_{ad} did not change between 200 and 400 K, but above 400 K, NO decomposition started (because no O_{ad} was present, which would otherwise inhibit NO_{ad} decomposition). As a result, the NO_{ad} concentration dropped. It is important to note that only a part of the N_{ad} formed NO_{ad}, whereas an equal part did not react and was present as N_{ad}.

In the gas phase, both H_2O and N_2 formation were observed between 400 and 600 K. The N-selectivity of the reaction changed above 600 K from N_2(g) to NO(g). The surface was almost empty at this temperature; that is, the NH_{xad}, NO_{ad}, and O_{ad} concentrations were almost zero. Due to experimental limitations, we were not able to observe the surface coverage above this temperature.

The change in N-selectivity was accompanied by a decrease in H_2O(g) formation. According to the overall reaction equations (1) and (2), more oxygen is needed for the formation of NO and H_2O than for formation of N_2 and H_2O. The ratio of 1:1 used in this experiment means that only a relatively small amount of oxygen was available, too little to oxidize all of the NH_3 to NO. As a result, the NH_3 conversion dropped above 600 K. In other words, the reaction rate during NO + H_2O formation decreased due to a lack of oxygen:

$$4NH_3 + 3O_2 \rightarrow 2N_2 + 6H_2O, \quad (1)$$

$$4NH_3 + 5O_2 \rightarrow 4NO + 6H_2O. \quad (2)$$

The cooling branch provides a better source of information about the steady-state reaction, because non-steady-state effects, caused by desorption of adsorbates present at low temperature, are absent. Above 400 K, the reaction, as observed by the gas-phase products, proceeded in the same manner, and all essential features, including reaction rate, selectivity change (around 600 K), and starting/stopping of the reaction (around 400 K), were similar for the heating and cooling branches.

The surface composition as a function of temperature was slightly different in the cooling branch, specifically below

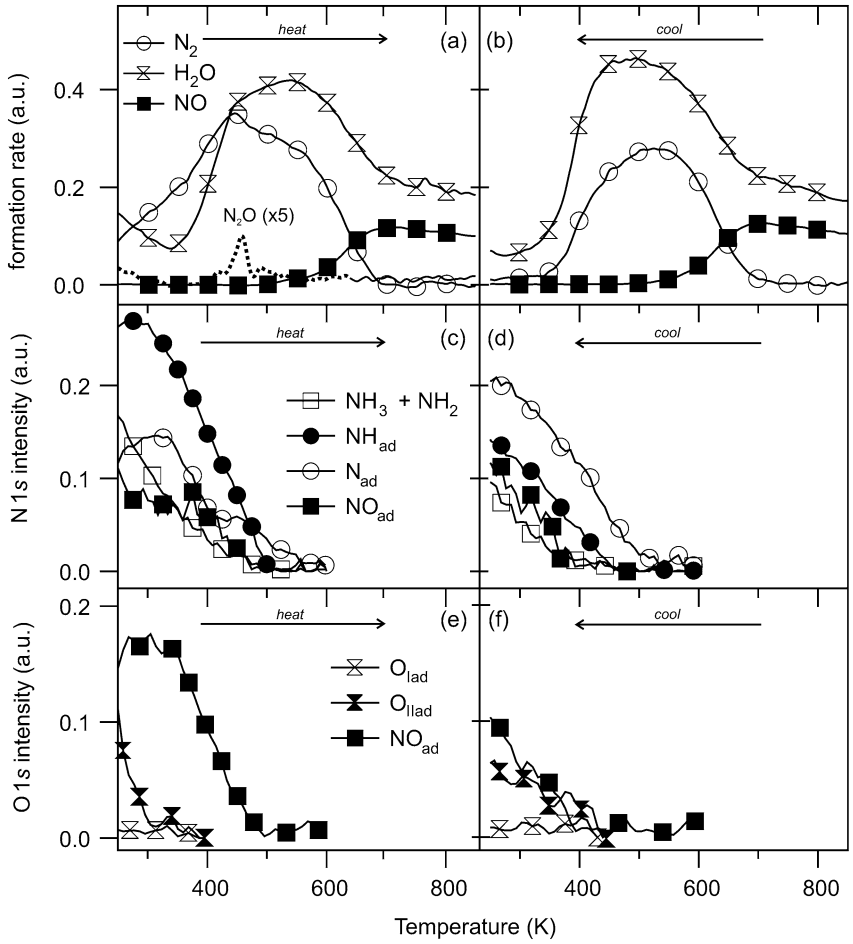

Fig. 7. Gas phase products (a, b) and surface coverage (c–f) during NH_3 oxidation on Pt(410), using a NH_3/O_2 ratio of 1:1. The heating and cooling branch are both shown ($pNH_3 = 1 \times 10^{-7}$ mbar (TPR)/5×10^{-8} mbar (XPS), NH_3:O_2 = 1:1, heating rate 0.5 K s^{-1} (TPR)/0.25 K s^{-1} (XPS)), 1 data point per ∼10 K.

∼500 K. The surface began to be covered by N_{ad} in the cooling branch, followed by NH_{ad}; at even lower temperatures, both NH_{3ad} ($+NH_{2ad}$) and NO_{ad} were observed. The amount of N_{ad} present in the cooling branch was larger than that in the heating branch, whereas the NH_{ad} and NH_{3ad} coverages were lower.

3.5.1. The influence of the reactant ratio

We also studied the effect of O_2 partial pressure on the reaction rate and selectivity. The results presented in Fig. 8 were obtained using an NH_3/O_2 ratio of 1:5, i.e., an excess of O_2. The NH_3 pressure was similar to the pressure used for the ratio 1:1, and the O_2 pressure was adjusted according to the desired ratio. The surface was precovered with O_{ad} before the reaction mixture was admitted.

The nature and abundance of the gas-phase products observed below ∼400 K in the first heating branch were the result of a complex combination of desorption of the initially present surface species and the products of steady-state reaction. N_2 formation showed two distinct peaks, one around 380 K and another one around 450 K. H_2O formation started at around 350 K, a similar temperature as for a reactant ratio of 1:1. The amount of water formed provides a good measure of the reaction rates for the two different ratios. For both ratios, the maximum H_2O formation occurred at around 500 K, and the amount of H_2O formation (i.e., the reaction rate) was about 1.5 times higher for the 1:5 ratio than for the 1:1 ratio. The greatest difference between the two ratios was the temperature at which the change in the N-selectivity occurred. For a ratio of 1:1, the selectivity changed at around 600 K, whereas for a ratio of 1:5, the selectivity changed at around 450 K. Because of the large amount of O_2 present, the H_2O formation for a ratio of 1:5 was not influenced by the selectivity change, in contrast to what we observed for a ratio of 1:1. Above 800 K, the reaction rate dropped. This is explained by the fact that O_{ad} starts to desorb (as O_2) (see Section 3.2), resulting in a lower O_{ad} concentration, and thus a lower reaction rate. A small peak was also observed for $m/e = 44$ between 400 and 500 K, somewhat higher than the $m/e = 44$ desorption peak found for a ratio of 1:1. We tentatively assign this peak to N_2O formed via reaction between N_{ad} and NO_{ad}.

In the cooling branch, only the products of the steady-state reaction were observed. During cooling, N_2 formation showed only a single peak, at around 420 K. The N_2 desorption peak observed at around 380 K in the heating branch is therefore assigned to a transient desorption peak, due to desorption of N_{ad} already present on the surface at lower temperature.

The results of the XPS measurements are shown in Figs. 8c–8f. The thermal behavior of the different NH_{xad} species was

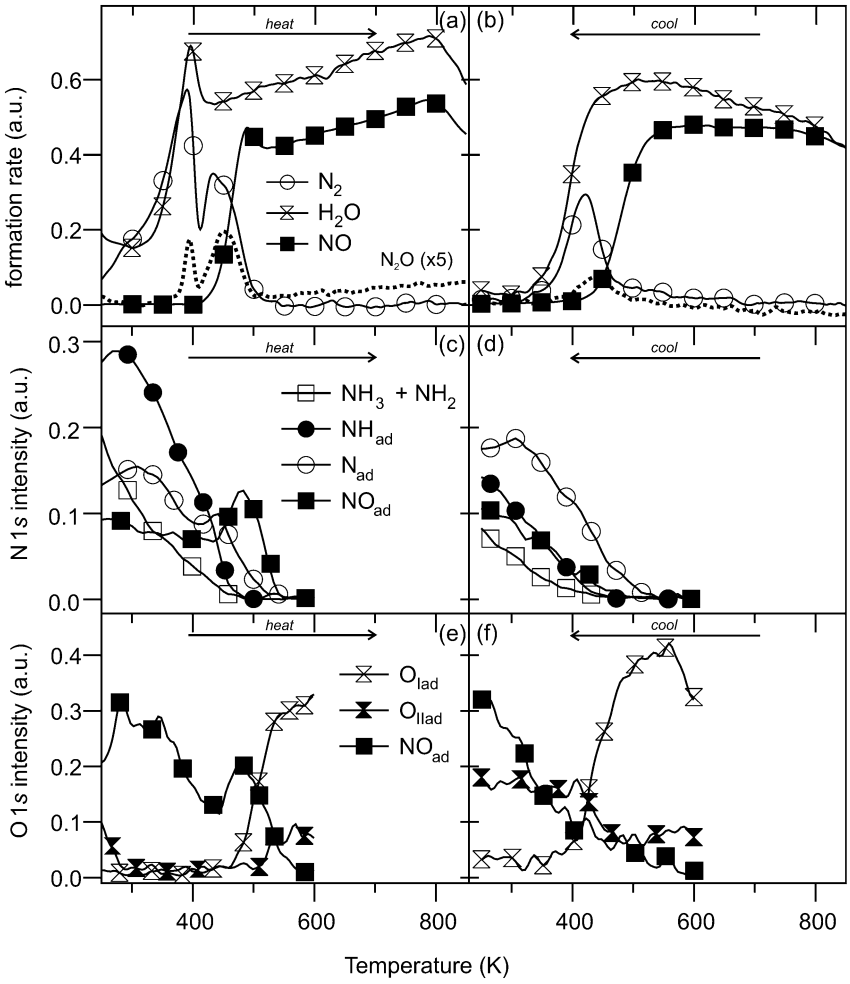

Fig. 8. Gas phase products (a, b) and surface coverage (c–f) during NH_3 oxidation on Pt(410), using a NH_3/O_2 ratio of 1:5. The heating and cooling branch are both shown (TPR: 0.5 K s^{-1}, 1×10^{-7} mbar NH_3, TP-XPS: 0.25 K s^{-1}, 5×10^{-8} mbar NH_3, 1 data point per ∼10 K).

very similar for both NH_3/O_2 ratios (1:1 and 1:5), whereas the NO_{ad} concentration was rather different for both ratios. For the ratio 1:5, NO_{ad} was present between 200 and 450 K; at 450 K, its concentration increased, reaching a maximum at around 480 K. For higher temperatures, the NO_{ad} concentration decreased again. NO_{ad} *dissociation* did not occur when a ratio of 1:5 was used, because O_{ad} was present on the surface above ∼450 K, and it inhibited NO_{ad} dissociation.

The O 1*s* spectral region shows a large difference between the two ratios. For the 1:5 ratio, the surface became O_{ad}-covered at around 450 K, in contrast to what was found for a 1:1 ratio. The change in surface coverage (from $NH_{x}ad$-to O_{ad}-covered) found for the 1:5 ratio coincides with the N-selectivity change in the gas phase. This shows that the selectivity of the NH_3 oxidation reaction on Pt(410) was determined by the surface coverage; when the surface was $NH_{x}ad/N_{ad}$-covered, the reaction product was mainly N_2, but when the surface was O_{ad}-covered, NO was the major product. The small amount of N_2O observed was formed only when both N_{ad} and NO_{ad} coexisted on the surface. This suggests that it formed via a reaction between N_{ad} and NO_{ad}.

The nature and concentration of the surface species in the cooling branch also differed from that in the heating branch. A hysteresis was observed in the O_{ad} concentration; that is, O_{ad} was observed on the surface down to 400 K, whereas in the heating branch O_{ad} was observed only above 500 K. This also influenced the $NH_{x}ad$ chemistry; more N_{ad} than NH_{ad} was present on the surface in the cooling branch.

4. General discussion

Thermal desorption spectra of NH_3 co-adsorbed with O_{ad} showed some N_2(g) formation already around 200 K, similar to the low-temperature N_2 desorption peak observed for Pt(100) [11] but significantly less than N_2 desorption from Pt(111) (>400 K), as observed by Mieher and Ho [3]. A similar trend was observed for NO_{ad} formation. Kim et al. found that NO_{ad} formation started at around 300 K on Pt(100). We found that NO_{ad} formation started at between 200 and 300 K on Pt(410). On Pt(111), on the other hand, the formation of NO_{ad} was not detected at all by EELS, whereas NO(g) was observed above 400 K [3]. These results indicate a special reactivity of the {100} facets of Pt, for several elementary steps in the NH_3 oxidation mechanism. Recent density functional theory (DFT) calculations [39,40] indicated that the activation energies for N_{ad} combination and NO_{ad} formation were much lower

on (bulk-terminated) Pt(100) and Pt(410) (∼90 and ∼70 meV per molecule, respectively) than on other Pt surfaces. Therefore, we explain the low-temperature N_2 desorption and the low-temperature NO_{ad} formation by the fact that the activation barriers associated with these processes are much lower on Pt(410) than on, for example, Pt(111).

Several authors have investigated steady-state NH_3 oxidation on stepped Pt single crystal surfaces, including Pt(533) [4-atom-wide {111} terraces, {100} steps], Pt(443) [7-atom-wide {111} terraces, {111} steps] and Pt(S)-12(111)×(111) [2,41,42]. The general trend found for all these surfaces is that $N_2 + H_2O$ forms at low temperatures, whereas $NO + H_2O$ forms at high temperatures. The exact temperature at which the N-selectivity changes varies for the different surfaces. Comparison between the different surfaces is complicated by the fact that the experimental conditions vary significantly. Scheibe et al. studied both Pt(533) and Pt(443), using similar reaction conditions for both surfaces and concluded that Pt(533) is more active than Pt(443). They offered two explanations for this difference: (i) the step density is higher for Pt(533) or (ii) the nature of the steps is different; that is, the {100} steps on Pt(533) are particularly reactive. In view of the preceding discussion, we support the second model.

In 2003, Günther et al. [43] published a *high-pressure* (∼ mbar) XPS study of ammonia oxidation on Pt(533) [{111} terraces, {100} steps]. They reported several peaks in the N 1*s* region, very similar to the peaks that we found on Pt(410). They also found that the NH_{xad} chemistry on the surface was similar at both low and high reactant pressures. These results show that low-pressure studies like ours are also relevant for understanding catalysis at industrially relevant pressures.

In a recent publication, we reported our results on NH_3 oxidation on Ir(110) and Ir(111) [9,13,14]. On Ir(110), we found that the change of surface composition from N_{ad}-covered to O_{ad}-covered occurred at significantly lower temperatures ($\Delta T \sim 200$ K) than the change in gas-phase selectivity. This was explained by a difference between the activation energies between N_2 formation and NO formation on Ir(110). On Pt(410), we showed that the change in surface coverage correlates with the change in gas-phase selectivity. Therefore, in the case of Pt(410), the gas-phase selectivity is governed by the surface coverage rather than by any difference in activation energy.

These kinetic considerations cannot be extended directly to other Ir and Pt facets, because the surfaces used in this case both demonstrate some *special* behavior. The activation barriers associated with N_2 and NO formation are much lower on Pt(410) than on other Pt surfaces, which should be kept in mind when applying insights obtained on surfaces containing {100} facets [like Pt(100), Pt(410), and Pt(533)] to other surfaces. On Ir(110), the presence of O_{ad} has a large effect on the N_2 formation rate [44].

Thermodynamic considerations offer a different, more general explanation for the different selectivities for Pt and Ir catalysts. These considerations are based on literature data regarding the (111) surfaces of Pt and Ir. Both O_{ad} desorption (as O_2) and N_{ad} desorption (as N_2) occur at a higher temperature (+300 K for O_{ad} and +50 K for N_{ad}) from Ir(111) than from Pt(111) [14,45–47], whereas NO desorption occurs at around the same temperature on both surfaces [45,48]. On Pt surfaces, NO_{ad} formation from N_{ad} and O_{ad} was found to be exothermic [39,40], which is the driving force for NO_{ad} formation on Pt. Ir(111) interacts more strongly with the atomic adsorbates (as shown by the higher N_2 and O_2 desorption temperatures), implying that NO_{ad} formation is less exothermic on Ir(111) than on Pt(111). As a result Ir(111) is less active for NO formation (and more active for NO dissociation) than Pt(111).

5. Conclusion

This study has investigated several elementary steps occurring during NH_3 oxidation on Pt(410). Ammonia adsorbs molecularly on Pt(410) and desorbs between 200 and 450 K. Radiation can induce dissociation, and several NH_{xad} surface species have been observed. NH_{ad} was found to be the most abundant (and probably most stable) surface species; it dissociates above 350 K. The N_{ad} (and H_{ad}) formed immediately desorb as N_2 (and H_2).

O_2 adsorbs both molecularly and dissociatively on Pt(410). Heating of an adsorbed O_2/O_{ad} layer results in O_2 desorption at around 160 K. The atomic oxygen desorbs (as O_2) in two steps at around 650 and 800 K. The O 1*s* core level spectra show both O_{2ad} and *two* O_{ad} species. In the presence of H_2, the formation of H_2O_{ad} occurs at around 150 K. H_2O_{ad} desorbs above 200 K.

The presence of O_{ad} enhances NH_{3ad} dissociation. Hydrogen abstraction starts at around 150 K, and H_2O_{ad} formed in this process desorbs above 200 K. N_2 desorption occurs between 200 and 500 K. NO_{ad} and NO(g) formation are also observed, but only during experiments where a large amount of O_{ad} is available. NO_{ad} desorbs/decomposes between 400 and 500 K, and both NO(g) and N_2(g) are observed in this temperature region.

The steady-state reaction between NH_3 and O_2 leads to N_2 and H_2O formation, but at higher temperature the selectivity changes toward NO and H_2O. The exact temperature at which the selectivity change occurs depends strongly on the reactant ratio. The selectivity change is accompanied by a change in surface coverage; N_2 is formed when the surface is NH_{xad}-covered, and NO is formed when the surface is O_{ad}-covered. We have compared our results with literature data for other Pt surfaces as well as results obtained on Ir surfaces. We propose that the main difference between Pt and Ir catalysts lies in the lower NO *formation* rate on Ir, rather than in a higher NO *decomposition* rate.

Acknowledgments

The authors acknowledge ELETTRA and the European Union for financial support for measurements at the Super-ESCA beamline of ELETTRA. They thank S. Lizzit, L. Petaccia, and A. Baraldi for their help during the beam time, and R.C.V. van Schie for his invaluable technical support. C.J.W., A.V.M., and V.V.G. acknowledge the Netherlands Technology foundation STW, the applied science division of NOW, and the technology program of the Ministry of Economic Affairs for

financial support under project UPC.5037. A.V.M. and V.V.G. also acknowledge the NWO Russia program for financial support under project number 047-015-002.

References

[1] J.L. Gland, E.B. Kollin, Surf. Sci. 104 (1981) 478–490.
[2] J.L. Gland, V.N. Korchak, J. Catal. 53 (1978) 9–23.
[3] W.D. Mieher, W. Ho, Surf. Sci. 322 (1995) 151–167.
[4] D.G. Löffler, L.D. Schmidt, Surf. Sci. 59 (1976) 195–204.
[5] J.M. Gohndrone, C.W. Olsen, A.L. Backman, T.R. Gow, E. Yagasaki, R.I. Masel, J. Vac. Sci. Technol. A 7 (3) (1989) 1986–1990.
[6] D.M. Thornburg, R.J. Madix, Surf. Sci. 220 (1990) 268–294.
[7] A. Fahmi, R.A. van Santen, Z. Phys. Chem. 197 (1996) 203–217.
[8] B. Afsin, P.R. Davies, A. Paskusky, M.W. Roberts, D. Vincent, Surf. Sci. 284 (1993) 109–120.
[9] C.J. Weststrate, J.W. Bakker, E.D.L. Rienks, S. Lizzit, L. Petaccia, A. Baraldi, C.P. Vinod, B.E. Nieuwenhuys, Phys. Chem. Chem. Phys. 7 (13) (2005) 2629–2634.
[10] M. Baerns, R. Imbihl, V.A. Kondratenko, R. Kraehnert, W.K. Offermans, R.A. van Santen, A. Scheibe, J. Catal. 232 (2005) 226–238.
[11] J.M. Bradley, A. Hopkinson, D.A. King, J. Phys. Chem. 99 (1995) 17032–17042.
[12] C.J. Weststrate, J.W. Bakker, E.D.L. Rienks, C. Vinod, S. Lizzit, L. Petaccia, A. Baraldi, B.E. Nieuwenhuys, Surf. Sci. 600 (10) (2006) 1991–2001.
[13] C.J. Weststrate, J.W. Bakker, E.D.L. Rienks, S. Lizzit, L. Petaccia, A. Baraldi, C.P. Vinod, B.E. Nieuwenhuys, J. Chem. Phys. 122 (18) (2005) 184705.
[14] C.J. Weststrate, J.W. Bakker, E.D.L. Rienks, J.R. Martinez, S. Lizzit, L. Petaccia, A. Baraldi, C.P. Vinod, B.E. Nieuwenhuys, J. Catal. 235 (2005) 92–102.
[15] S.A.C. Carabineiro, B.E. Nieuwenhuys, Surf. Sci. 505 (2002) 163–170.
[16] S.A.C. Carabineiro, B.E. Nieuwenhuys, Surf. Sci. 532 (2003) 87–95.
[17] A. Baraldi, G. Comelli, S. Lizzit, M. Kiskinova, G. Paolucci, Surf. Sci. Rep. 49 (6–8) (2003) 169–224.
[18] A. Baraldi, M. Barnaba, B. Brena, D. Cocco, G. Comelli, S. Lizzit, G. Paolucci, R. Rosei, J. Electron Spectrosc. Relat. Phenom. 76 (1995) 145–149.
[19] A. Baraldi, G. Comelli, S. Lizzit, D. Cocco, G. Paolucci, R. Rosei, Surf. Sci. 367 (3) (1996) L67–L72.
[20] J.J. Joyce, M. del Guidice, J.H. Weaver, J. Electron Spectrosc. Relat. Phenom. 49 (1) (1989) 31–45.
[21] Y.-M. Sun, D. Sloan, H. Ihm, J.M. White, J. Vac. Sci. Technol. A 14 (3) (1996) 1516–1521.
[22] A.L. Schwaner, E.D. Pylant, J.M. White, J. Vac. Sci. Technol. A 14 (3) (1996) 1453–1456.
[23] G.B. Fisher, Chem. Phys. Lett. 79 (3) (1981) 452–458.
[24] C. Benndorf, T.E. Madey, Surf. Sci. 135 (1–3) (1983) 164–183.
[25] D.R. Jennison, P.A. Schultz, M.P. Sears, Surf. Sci. 368 (1996) 253–257.
[26] B.A. Sexton, G.E. Mitchell, Surf. Sci. 99 (1980) 523–538.
[27] G.J. Szulczewski, J.M. White, Surf. Sci. 406 (1998) 194–205.
[28] N. Freyer, M. Kiskinova, G. Pirug, H.P. Bonzel, Surf. Sci. 166 (1986) 206–220.
[29] A. Rar, T. Matsushima, Surf. Sci. 318 (1994) 89–96.
[30] K. Schwaha, E. Bechtold, Surf. Sci. 65 (1977) 277–286.
[31] N.R. Avery, Chem. Phys. Lett. 96 (3) (1983) 371–373.
[32] J.L. Gland, B.A. Sexton, G.B. Fisher, Surf. Sci. 95 (1980) 587–602.
[33] Y. Ohno, T. Matsushima, Surf. Sci. 241 (1–2) (1991) 47–53.
[34] G.B. Fisher, J.L. Gland, Surf. Sci. 94 (1980) 446–455.
[35] M.A. Henderson, Surf. Sci. Rep. 46 (2002) 1–308.
[36] M. Kiskinova, G. Perug, H.P. Bonzel, Surf. Sci. 150 (1985) 319–338.
[37] W.K. Offermans, A.P.J. Jansen, R.A. van Santen, Surf. Sci. 600 (2006) 1714–1734.
[38] M. Kim, S.J. Pratt, D.A. King, J. Am. Chem. Soc. 122 (2000) 2409–2410.
[39] A. Eichler, J. Hafner, J. Catal. 204 (2001) 118–128.
[40] Q. Ge, M. Neurock, J. Am. Chem. Soc. 126 (2004) 1551–1559.
[41] A. Scheibe, U. Linz, R. Imbihl, Surf. Sci. 577 (2005) 1–14.
[42] A. Scheibe, U. Linz, R. Imbihl, Surf. Sci. 577 (2005) 131–144.
[43] S. Günther, A. Scheibe, D. Albrecht, R. Imbihl, H. Bluhm, M. Mävecker, A. Knop-Gericke, E. Kleimenov, BESSY Annu. Rep. (2003) 274–276.
[44] C.A. de Wolf, J.W. Bakker, P.T. Wouda, B.E. Nieuwenhuys, A. Baraldi, S. Lizzit, M. Kiskinova, J. Chem. Phys. 113 (2000) 10717–10722.
[45] J.C.L. Cornish, N.R. Avery, Surf. Sci. 235 (1990) 209–216.
[46] D.M. Collins, J.B. Lee, W.E. Spicer, Surf. Sci. 55 (1976) 389–402.
[47] K. Schwaha, E. Bechtold, Surf. Sci. 66 (1977) 383–393.
[48] R.J. Gorte, L.D. Schmidt, J.L. Gland, Surf. Sci. 109 (1981) 367–380.